

Bathocuproine Buffer Layer Effect on the Performance of Inverted Perovskite Solar Cells

Naïma Touafek^{1,*}, Chahrazed Dridi² and Ramdane Mahamdi³

¹Higher National School of Biotechnology "Toufik Khaznadar" (ENSB), Constantine, Algeria

²LPMS, Mentouri brothers, Constantine1 University, Algeria

³LEA, Department of electronic, University of Batna2, Algeria

Abstract: To boosting the performance of inverted p-i-n-type planar hetero-junction architecture photovoltaic cells based on $\text{CH}_3\text{NH}_3\text{PbI}_3$ perovskite materials, a thin buffer layer Bathocuproine (BCP) is introduced between the Electron Transporting Layer (ETL) PCBM and the metal contact. The trends in parameters Perovskite Solar Cells (PSCs) inserting BCP is studied using solar cell capacitance simulator (SCAPS-1D). The obtained results of optimizing the thickness of the Bathocuproine (BCP) buffer layer exhibited optimum value at 5 nm, with power conversion efficiency (PCE) of 17.30 %, V_{oc} of 1.39 V, and FF of 62.89 %. The carrier concentration was higher than 10^{17} cm^{-3} increases sharply the conversion efficiency by about 0.35-2.3 %. Further, the lower metal work function ($\Phi_m < 4.3 \text{ eV}$) enhances the electrical parameters where the efficiency up to 21.3 %.

Keywords: Solar cell, Perovskite, $\text{CH}_3\text{NH}_3\text{PbI}_3$, BCP, SCAPS, Metal Work Function.

1. INTRODUCTION

Thin-film technologies (TFTs) permit to save material, decrease the processing time, the energy needed to produce the solar cell and therefore decrease the production cost. Perovskites are part of research context for new materials in thin layers. These emerging semiconductors have many qualities that make it possible to consider it as a credible alternative to other thin-film technologies such as: amorphous silicon, CIGS, and CdTe. The 26.1% [1] conversion efficiency obtained in Perovskites Solar Cells (PSCs) is encouraging and is considered as an interesting stimulant for the development of PSCs devices. Perovskite belongs to a class of compounds which have an ABX crystal structure, A and B are two cations of very different sizes and X is an anion, typically oxygen, halogens, or alkali metals. PSCs devices are commonly based on organo-lead or organo-tin halide perovskites as light-absorber semiconductors such as $\text{CH}_3\text{NH}_3\text{PbI}_3$, denoted as MAPbI_3 , and $\text{CH}_3\text{NH}_3\text{SnI}_3$, respectively. The perovskite material worked not only as a light-absorber but also as a hole and electron transporter [2], due to this ambipolar semiconducting characteristic the perovskites solar cells can be designed in two planar configurations:

➤ n-i-p conventional structure: the Electron Transport Layer (ETL) connected to the front surface electrode, and the Hole Transport Layer (HTL) connected to the rear surface electrode.

➤ p-i-n inverted structure: in this configuration, the HTL connected to the front surface electrode and the ETL connected to the rear electrode.

In inverted planar Perovskites Solar Cells, the Electron Transport Layers (ETLs) such as fullerene (C60), [6,6]-Phenyl- C61-Butyric Acid Methyl Ester (PCBM) and derivatives play an important role to efficiently extract and transport the photogenerated electron from the perovskite absorber to the metal electrode [3,4]. However, due to the high work function of the metal electrode, a large electron contact barrier appears at the PCBM / Metal interface, which results in severe interfacial carrier accumulation resulting in deteriorated device performance [5].

To prevent recombination between the electron transport layer and the metal electrode to boosting the performance of perovskite solar cells, an extremely thin buffer layer that acts both as an exciton blocking (EBL) and electron transporting (ETL) such as Bathocuproine (BCP), LiF or Ti (Nb)Ox [6,7] is required.

Bathocuproine (BCP), an organic semiconductor, is an electron transport material having an energy difference of 3.5 eV between the highest occupied molecular orbital (HOMO) and the lowest unoccupied molecular orbital (LUMO) [8]. It is used as a hole-blocking layer between the PCBM and the metal cathode to improve the cell performance [9], however, has not been clearly understood for complex features such as formation of an interfacial dipole layer and gap states due to the interaction at the BCP/metal interfaces [10].

Address correspondence to this author at the Ville University Ali Mendjeli, Boite Postale E66 Constantine (Population range: 250,000-499,999) 25100 Constantine, Algeria; Tel: 21331786011; E-mail: ntouafek@yahoo.fr

In this work, using SCAPS-1D simulation package [11], the goal is to study the effect of the presence of the BCP buffer layer on the photovoltaic output parameters of $\text{CH}_3\text{NH}_3\text{PbI}_3$ absorber solar cells. We examine the influence of the BCP layer thickness, the carrier density, as well as the effect of the type of the metal electrode on the performance.

2. MATERIALS AND METHODS

2.1. Structure of Solar Cell

Figure 1 shows a schematic of a typical inverted p-i-n-type planar hetero-junction architecture used in this study with the energy band diagram. The cell structure consists of fluorine-doped tin oxide ($\text{Sn}_2\text{O}_3:\text{F}$) as the transparent conductive layer (front contact), a p-type NiMgLiO layer as the hole transport layer (HTL) which promoted ohmic contact formation at the $\text{FTO}/\text{MAPbI}_3$ interface, an organo-halide perovskite $\text{CH}_3\text{NH}_3\text{PbI}_3$ as the absorber layer, an n-type PCBM layer as the electron transport layer (ETL), an n-type BCP buffer layer and a metallic Ag back contact complete the cell.

2.2. Numerical Modelling

In this work, we have used a simulation program called Solar Cell Capacitance Simulation in 1 Dimension (SCAPS-1D) to predict the changes to $\text{CH}_3\text{NH}_3\text{PbI}_3$ based solar cell performance that are introduced by the presence of the BCP buffer layer between the PCBM and the metal contact. This numerical simulation programme developed at the Department of Electronics and Information Systems (ELIS) of the University of Gent, Belgium [11], is used to analyze the micro and polycrystalline and photonic structure, allows the definition of thin-film solar cell devices stacks of layers with a large set of parameters and solves for each point the fundamental solar cell equations: the Poisson equation and the continuity

equations for electrons and holes. To describe the recombination currents in deep bulk levels, the Shockley-Read-Hall (SRH) model is used. However, an extension of this model describes the defects at the interfaces [11]. The series and shunt resistances are taken in to account in this study with values vary with the thickness of the BCP buffer layer [12]. The defect level of the absorber layer is positioned at the mid band-gap; the absorption coefficient of $\text{CH}_3\text{NH}_3\text{PbI}_3$ is adopted from Duong's work [13]. All simulations in this work were performed under illumination standard spectrum AM1.5 and ambient temperature (300 K). The metal electrode in the two first simulation results sections (3.1 and 3.2) is chosen to have a work function of 4.26 eV (Ag) with a surface recombination velocity of 10^7 cm/s and 10^5 cm/s for electrons and holes, respectively. The physical parameters used for the simulation are all extracted from the experimental procedures and numerical models [8, 11-13].

3. RESULTS AND DISCUSSIONS

In order to validate our study, consistent comparison of our numerical study with an experimental one is necessary. The current-voltage (J-V) results from simulation using the parameters given in Table 1 without the BCP buffer layer, as well as the electrical parameters, are compared with measurement data from [12] in Figure 2 and Table 2, respectively. The results show that the measured J-V and the values of all electrical parameters are very well reproduced by the parameters model which validates our set of parameters as a baseline for simulating the effect of the BCP on the solar cell performance.

3.1. Modeling with Various BCP Thicknesses

The perovskite solar cell performance for different thickness of the BCP buffer layer (d_{BCP}) ranging from 1

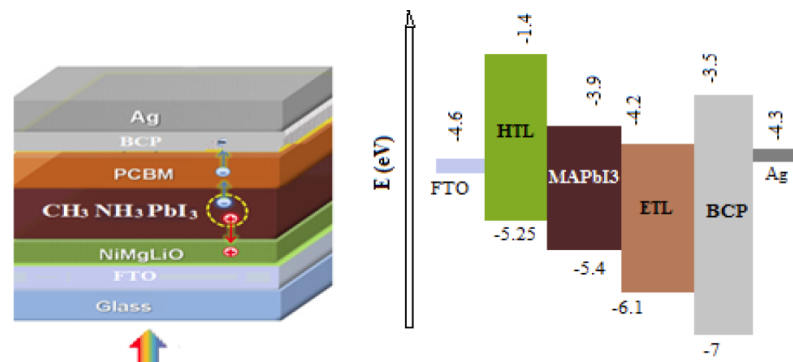
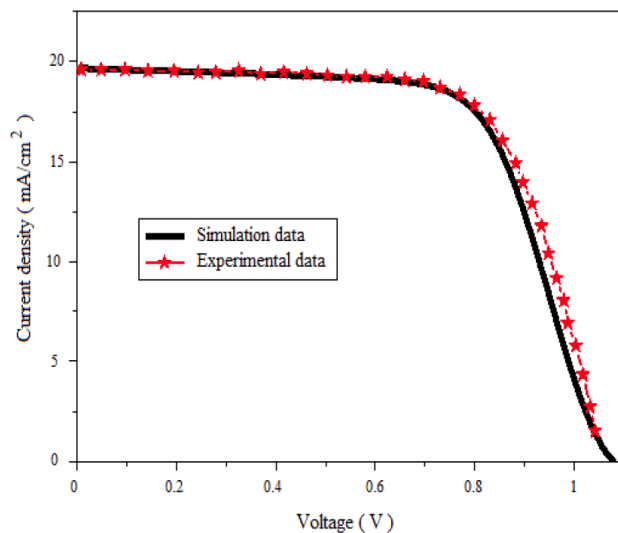


Figure 1: Schematic illustration of inverted type (p-i-n) planar hetero-junction $\text{CH}_3\text{NH}_3\text{PbI}_3$ perovskite solar cell and corresponding energy level diagram (layer thicknesses not to scale).

Table 1: Input Parameter Values for the Simulation of CH₃NH₃PbI₃ Perovskite Solar Cells with SCAPS-1D

	NiMgLiO	CH ₃ NH ₃ PbI ₃	PCBM	BCP
W(nm)	80	450	60	Var
E _g (eV)	2.2	1.55	2.1	3.5
χ (eV)	2.9	3.75	3.9	3.9
ε/ε ₀	3	6.5	3.9	4
N _c (cm ⁻³)	2.2*10 ¹⁵	2.2*10 ¹⁵	2.2*10 ¹⁹	2.2*10 ¹⁵
N _v (cm ⁻³)	1.8*10 ¹⁸	2.2*10 ¹⁷	2.2*10 ¹⁹	1.8*10 ¹⁷
v _n (cm/s)	1*10 ⁷	1*10 ⁷	1*10 ⁷	1*10 ⁷
v _p (cm/s)	1*10 ⁷	1*10 ⁷	1*10 ⁷	1*10 ⁷
μ _n (cm ² /Vs)	0.01	2	0.001	0.001
μ _p (cm ² /Vs)	0.0002	2	0.002	0.002
Doping (cm ⁻³)	1*10 ¹⁶ (A)	1*10 ¹³ (I)	1*10 ¹⁶ (D)	Var

**Figure 2:** Comparison between (J-V) curves for the simulated and the reported experimental data [12].

to 13 nm is studied. Changing of the all parameters in term of the open-circuit voltage (V_{OC}), the short circuit current density (J_{SC}), the Fill Factor (FF) and the conversion efficiency (η) are shown in Figure 3. The results exhibit the influence of the film thickness of the BCP buffer layer on the PSCs with an optimal value of efficiency equals to 17.30 % obtained at d_{BCP} = 5 nm. On the other hand, by decreasing furthermore the

thickness of the BCP below 5 nm, the performances of the device decrease sharply. At the same time, the short circuit current density (J_{SC}) remains nearly constant until 10 nm. We also noted that the FF and V_{oc} decrease with increasing the thickness of the BCP buffer layer from 5 nm to 13 nm by about 12.4 % and 0.25 V, respectively. This is mainly due to serious electron-hole recombination induced by charge accumulation occurs at the perovskite/PCBM interface and series resistance which increases by increasing the BCP thickness, thereby resulting in the decrease of the efficiency from 17.30 % for d_{BCP} = 5 nm to 10.86 % for d_{BCP} = 13 nm. For the lower thickness of BCP, the obtained results confirm that this buffer layer can prevent contact between the PCBM layer and the electrode, which improves the interface to a good ohmic contact. Attempts are made to compare the simulation results with reported experimental data [12] for the structure solar cell studied in this work. Good agreement was obtained between the simulation solar cell electrical parameters (V_{OC} , J_{SC} , FF, and conversion efficiency) trends and the experimental values. However, the simulation values are slightly higher than the experimental ones for the thickness higher than 8 nm. This difference can be attributed to the defect density at the PCBM / BCP interface, which was not considered in this work, especially for the V_{OC} , which

Table 2: Measured and Simulated Solar Cell J-V Parameters

	V_{oc} (mV)	J_{sc} (mA/cm ²)	FF (%)	η (%)
Simulation	1.0789	19.674	66.22	14.06
Experimental [12]	1.0710	19.670	66.00	14.07

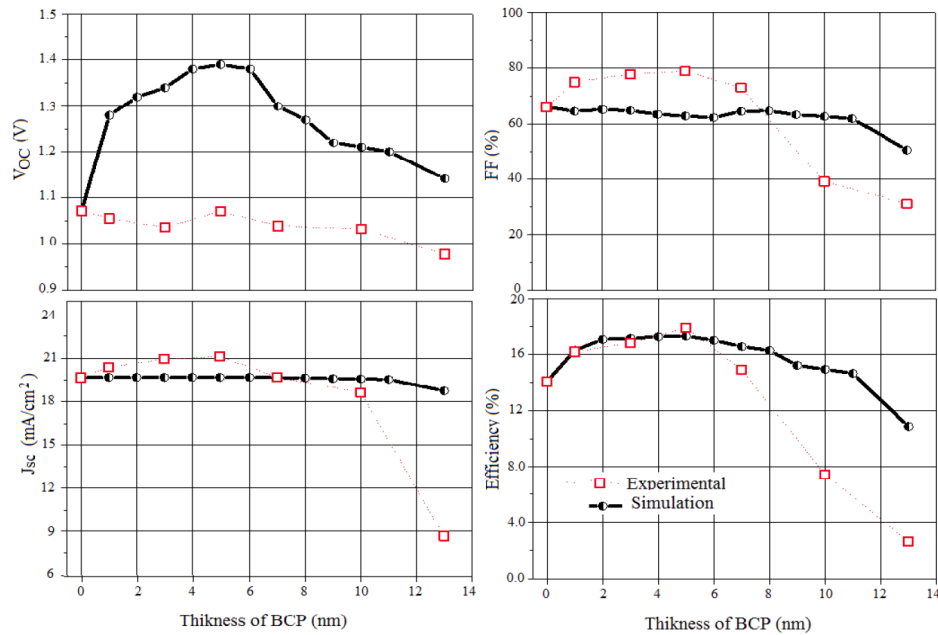


Figure 3: Graph representing variation of PV parameters, by varying the thickness of the BCP (nm). The solid red circles denote the experimental data extracted from [12].

should be ascribed to the high charge recombination rate in the experimental values.

3.2. Modeling with Various BCP Carrier Density

The dependence of BCP's donor concentration (N_D) on the PV parameters of the cell has been investigated. To understand the carrier density effect of the BCP on the device performance, this parameter is varied from

10^{14} to 10^{20} cm^{-3} , and the thickness of the BCP is fixed at the optimal value, $d_{\text{BCP}}=5$ nm. Figure 4 represents the changes in the PV parameters as function of the BCP carrier density. For all parameters, except J_{sc} which remains nearly constant, we can distinguish two zones of the carrier concentration. The first zone is $N_D < 10^{17}$ cm^{-3} , where all parameters look a constant behavior because the carrier density is not sufficient to improve the interface to a good ohmic contact.

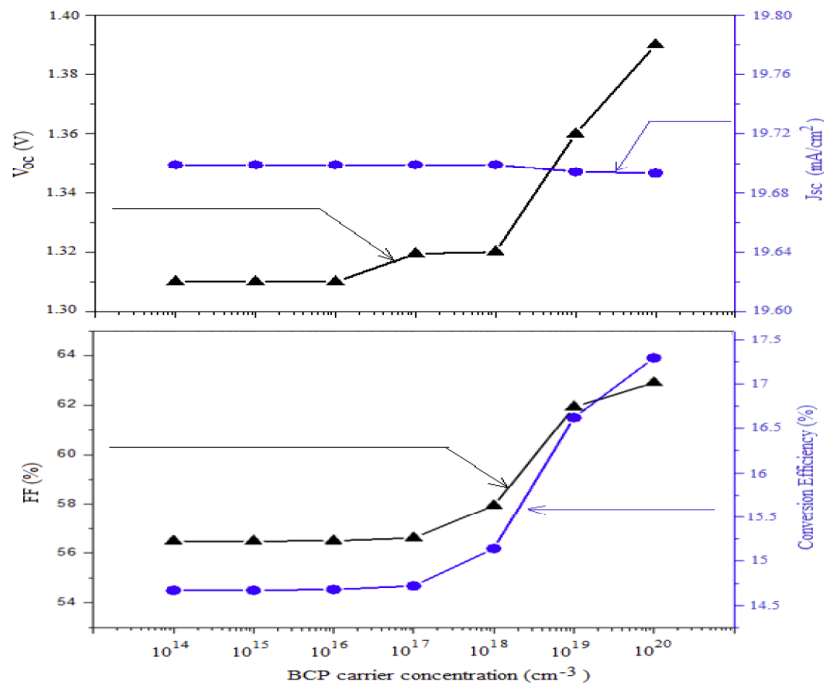


Figure 4: Performance device as function of the BCP carrier concentration.

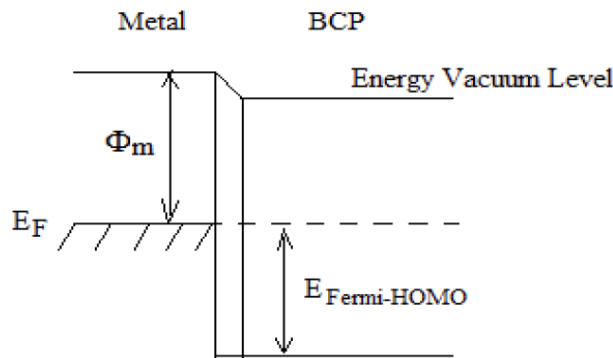


Figure 5: Energy level diagram of the BCP on the metal cathode.

In the second zone corresponds to $N_D > 10^{17} \text{ cm}^{-3}$, the V_{OC} , FF, and conversion efficiency are strongly influenced by the augmentation of the carrier density in the BCP buffer layer. The V_{OC} passes from 1.32 V for $N_D=10^{18} \text{ cm}^{-3}$ to 1.39 V for $N_D=10^{20} \text{ cm}^{-3}$ due to the formation of a better ohmic contact between the BCP buffer layer and the electrode. For the FF and conversion efficiency the influence is more pronounced where we noted an augmentation of 6.3 % and 2.6 %, respectively, when the carrier density changes from 10^{17} to 10^{20} cm^{-3} .

3.3. Modeling with Various Types of Metals as Electrode

The energy level alignment at the BCP/metal interface was found to depend on the metal work function [10]. So understanding the effect of the type of the metal constituted the electrode on the performance of the device is very important to reach maximum efficiency. For this purpose, the work function of the metal electrode was varied between 2.9 and 4.7 eV. The thickness and the carrier concentration of the BCP are fixed at 5 nm and 10^{20} cm^{-3} , respectively, while the other parameters of all layers of solar cell were kept constant.

Figure 5 shows the energy level diagram of the BCP on the metal cathode. Φ_m represents the work function of the metal used as an electrode; $E_{\text{Fermi-HOMO}}$ determines the HOMO energy level of the BCP with respect to the Fermi level (E_F).

With decreasing the work function (Φ_m), the $E_{\text{Fermi-HOMO}}$ approaches to the HOMO-LUMO energy gap of the BCP (3.5 eV), which makes the LUMO energy level of the BCP very close to the E_F , that is, the electron is easily transferred from the metal (E_F) to the BCP

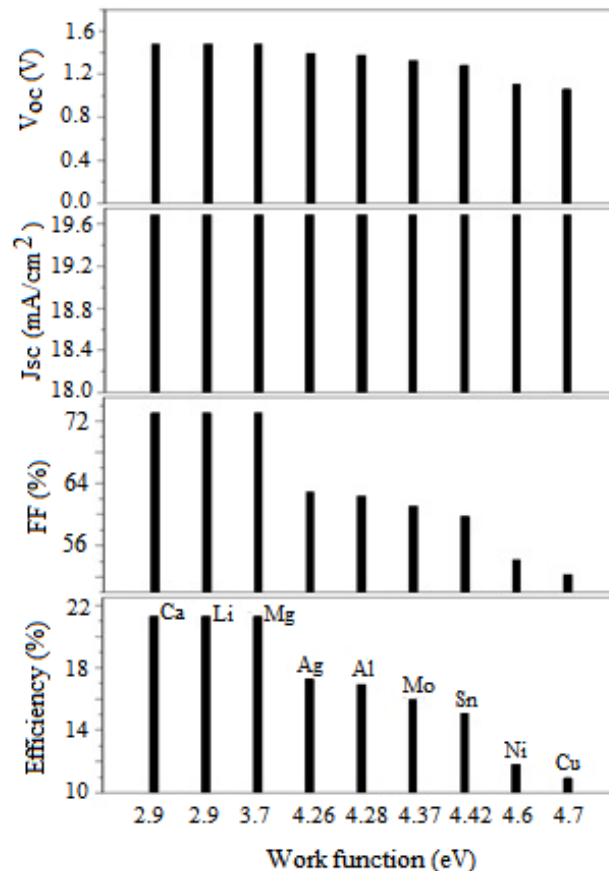


Figure 6: Solar cell parameters as function of metal electrode work function.

(LUMO) due to the disappearance of the electron injection barrier. Whereas, increasing the metal work function (Φ_m) leads to an increase in the difference between the E_F and the LUMO level which affects the transfer of the electrons from metal to the LUMO due to the appears of the injection barrier.

For an electrode contact work function $\Phi_m < 4.3$ eV such as Mg, Li, Ca and Ag, the results, depicted in Figure 6, exhibit high electrical parameters, with an efficiency up to 21.3 %, compared to the metals have $\Phi_m > 4.3$ eV such as Cu, Ni and Sn where the conversion efficiency drops to 10.94 %.

4. CONCLUSIONS

The numerical simulation tool SCAPS-1D was used to analyze perovskite solar cells having the architecture FTO/PCBM/CH₃NH₃PbI₃/NiMgLiO/Ag contains inverted planar hetero-junction device. In this work, the trends in PSCs inserting a BCP buffer layer between the PCBM (ETL) and the metal electrode is studied. Simulation results show that an optimal thickness equal 5 nm of the BCP layer is showing the better performance. We got the power conversion efficiency is 17.30 %, a good V_{OC} value (1.39 V) is attained and the corresponding FF is 62.89 %. On the other hand, it was found that an excessive BCP film thickness deteriorates the PCE by about 6.5 %. We have also shown that the device performance for a high carrier density is better than with a low one. Increasing the carrier density beyond 10^{17} cm⁻³ enhances the V_{OC} , FF, and efficiency by about 0.01-0.07 V, 1.3-6.3 %, and 0.35-2.6 %, respectively. We conclude from our numerical results that the type of the metal electrode also influences the performance of the device. We note a high device performance for the metal electrode has a work function $\Phi_m < 4.3$ eV with an efficiency up to 21.3 %. However, the higher metal work function deteriorates the performance of PSCs where the efficiency drops to 10.94 %.

ACKNOWLEDGEMENT

We acknowledge the use of SCAPS-1D program developed by Marc Burgelman and colleagues at the University of Gent in all the simulation reported in the paper.

REFERENCES

- [1] National Renewable Energy Laboratory (NREL). Best research-cell efficiencies. Accessed on September 2020. <https://www.nrel.gov/pv/cell-efficiency.html>
- [2] Etgar L, Gao P, Xue Z, *et al.* Mesoscopic CH₃NH₃PbI₃/TiO₂ heterojunction solar cells. Journal of the American Chemical Society 2012; 134: 17396-17399. <https://doi.org/10.1021/ja307789s>
- [3] Luo D, Yang W, Wang Z, *et al.* Enhanced photovoltage for inverted planar heterojunction perovskite solar cells. Science 2018; 360: 1442-1446. <https://doi.org/10.1126/science.aap9282>
- [4] Groeneveld BGHM, Najafi M, Steensma B, Adjoktse S, *et al.* Improved efficiency of NiO_x-based p-i-n perovskite solar cells by using PTEG-1 as electron transport layer. APL Materials 2017; 5: 076103. <https://doi.org/10.1063/1.4992783>
- [5] Lo MF, Guan ZQ, Ng TW, Chan CY, Lee CS. Electronic structures and photoconversion mechanism in perovskite/fullerene heterojunctions. Advanced Functional Materials 2015; 25: 1213-1218. <https://doi.org/10.1002/adfm.201402692>
- [6] Heo JH, Han HJ, Kim D, Ahn TK, Im SH. Hysteresis-less inverted CH₃NH₃PbI₃ planar perovskite hybrid solar cells with 18.1% power conversion efficiency. Energy Environmental Science 2015; 8: 1602-1608. <https://doi.org/10.1039/C5EE00120J>
- [7] Seo J, Park S, Kim YC, *et al.* Benefits of very thin PCBM and LiF layers for solution-processed p-i-n perovskite solar cells. Energy Environmental Science 2014; 7: 2642-2646. <https://doi.org/10.1039/C4EE01216J>
- [8] Hill G, and Kahn A. Organic semiconductor heterointerfaces containing bathocuproine. Journal Applied Physics, 1999; 86: 4515. <https://doi.org/10.1063/1.371395>
- [9] Shibayama N, Kanda H, Kim TW, Segawa H, and Ito S. Design of BCP buffer layer for inverted perovskite solar cells using ideal factor. APL Materials 2019; 7: 031117. <https://doi.org/10.1063/1.5087796>
- [10] Sakurai T, Toyoshima S, Kitazume H, *et al.* Influence of gap states on electrical properties at interface between bathocuproine and various types of metals. Journal Applied Physics 2010; 107: 043707. <https://doi.org/10.1063/1.3309278>
- [11] Petterson J, Platzer-bjorkman C, Zimmermann U, Edoff M. Baseline model of graded-absorber Cu(In,Ga)Se₂ solar cells applied to cells with Zn_{1-x}Mg_xO buffer layers. Thin Solid Films 2011; 519: 7476-7480. <https://doi.org/10.1016/j.tsf.2010.12.141>
- [12] Chen C, Zhang S, Wu S, *et al.* Effect of BCP buffer layer on eliminating charge accumulation for high performance of inverted perovskite solar cells. RSC Advances 2017; 7: 35819. <https://doi.org/10.1039/C7RA06365B>
- [13] Duong T, Development of high efficiency four-terminal perovskite-silicon tandems. Thesis, Australian National University, Austria, Jan. 2017. https://www.researchgate.net/publication/321242980_Development_of_High_Efficiency_Four-Terminal_Perovskite-Silicon_Tandems#fullTextFileContent